The Impact of Data Boundaries upon a Successive Corrections Objective Analysis of Limited-Area Datasets

GARY L. ACHTEMEIER

Climate and Meteorology Section, Illinois State Water Survey, Champaign, IL 61820

(Manuscript received 10 January 1985, in final form 31 May 1985)

ABSTRACT

Successive corrections objective analysis techniques frequently are used to array data from limited areas without consideration of how the absence of data beyond the boundaries of the network impacts the analysis in the interior of the grid. This problem of data boundaries is studied theoretically by extending the response theory for the Barnes objective analysis method to include boundary effects. The results from the theoretical studies are verified with objective analyses of analytical data. Several important points regarding the objective analysis of limited-area datasets are revealed through this study.

(i) Data boundaries impact the objective analysis by reducing the amplitudes of long waves and shifting the phases of short waves. Further, in comparison with the infinite plane response, it is found that truncation of the influence area by limited-area datasets and/or the phase shift of the original wave during the first pass amplified some of the resolvable short waves upon successive corrections to that first pass analysis.

(ii) The distance that boundary effects intrude into the interior of the grid is inversely related to the weight function shape parameter. Attempts to reduce boundary impacts by producing a smooth analysis actually draw boundary effects farther into the interior of the network.

(iii) When analytical tests were performed with realistic values for the weight function shape parameters, such as the GEMPAK default criteria, it was found that boundary effects intruded into the interior of the analysis domain a distance equal to the average separation between observations. This does not pose a problem for the analysis of large datasets because several rows and columns of the grid can be discarded after the analysis. However, this option may not be possible for the analysis of limited-area datasets because there may not be enough observations.

The results show that, in the analysis of limited-area datasets, the analyst should be prepared to accept that most (probably all) analyses will suffer from the impacts of the boundaries of the data field.

1. Introduction

Field experiments often involve the collection of tropospheric data in networks of limited areal extent. The expense involved in obtaining upper air data usually restricts these networks to no more than 10–15 observing sites. Several limited-area tropospheric sampling networks have been operated during the last two decades to support meteorological research. The National Severe Storms Laboratory (NSSL) operated 8–10 rawinsonde sites during 1966–70 (Barnes *et al.*, 1971) and the number of sites ranged from three to nine during the last decade (Alberty *et al.*, 1977; Doviak, 1981; Taylor, 1982). Other networks operated in the last 15 years include: METROMEX, 10 pibal sites in 1971 (Changnon *et al.*, 1971) and 11 sites in 1973 (ISWS, 1974); SESAME, 20 storm-scale rawinsonde sites in 1979 (Hill *et al.*, 1979); and CCOPE, five rawinsonde sites in 1981 (News and Notes, 1981).

In the analysis of upper air data from limited-area networks with eight or more measuring sites, the analyst may prefer an objective interpolation of the data from the irregularly spaced observation sites to points on a regular grid. An approach to the interpolation of the data would be the use of a multivariate statistical interpolation method (Gandin, 1963; Schlatter, 1975) found to be useful for the analysis of large datasets with several interrelated parameters. However, such a technique requires both good first-guess fields and reliable models of the first-guess field error statistics. These are generally not available for limited-area networks. We can, however, use the simpler successive corrections methods such as the techniques of Cressman (1959) or Barnes (1964, 1973).

Regarding the objective interpolation of meteorological data, Eddy (1964) suggested that the analyst take into consideration the data density, the significant wavelengths in the field, the best method for interpolating between observation points, and the noise level in the data. For limited-area datasets, the analyst should also consider the extent to which the absence of observations beyond the boundaries of the data field causes the method to degrade the analysis of the waves defined within the interior of the network. This latter problem is the subject of this paper. We are not concerned with extrapolation, although extrapolation is

often unavoidable in the transferral of information from irregularly shaped data fields onto a regular grid. Instead, we are concerned with how an objective analysis technique responds to the presence of boundaries in a limited-area data field. We seek answers to the following questions: What impacts are measured at various wavelengths? How far do the impacts extend into the grid interior and what can be done to confine adverse impacts to an area near the grid boundaries?

The spectral responses of several objective interpolation techniques that use distance-dependent weight functions have been derived with the assumption either that the data were distributed continuously (Barnes, 1964) or that they were distributed uniformly upon a plane within an "influence radius" from some point of interpolation (Stephens, 1967; Stephens and Stitt, 1970). This response theory will be extended to assess the impact of the boundaries of the data field upon an objective analysis.

We will use the successive corrections method developed by Barnes (1964) and extended by him in 1973. This method has found widespread use in the analysis of regional scale and mesoscale phenomena, studies that most often involve the analysis of limited-area data fields. It is also the objective analysis technique in the GEMPAK program package (Koch *et al.*, 1983), which is being distributed widely within the meteorological community. Throughout the theoretical discussion, it is assumed that a continuum of information exists within the data field. In the real world this is never achieved; the response is degraded further by the discrete data distribution and is beyond the scope of this paper. However, the continuum response provides a baseline for the best analysis achievable near data boundaries.

In section 2 we formulate the problem and discuss the Barnes analysis technique in the context of first and second pass responses near data boundaries. Section 3 gives examples of the impact of data boundaries upon objective analyses of analytic data, and section 4 presents a discussion of the results.

2. Impact of data boundaries upon an objective analysis—Theoretical studies

The Barnes (1973) report has become an unofficial instruction manual for those who use his objective analysis method. Therefore, we will adhere to the original nomenclature and developments where possible and will also use original examples to demonstrate the impact of data boundaries upon the analysis.

Suppose an atmospheric variable can be described by a horizontal function $f(x, y)$. Assume a continuum of observations regarding $f(x, y)$, and filter (weigh) these data according to their distance from an arbitrary point (x, y). We wish to determine the relationship between observed value, f, and weighted average value, g, at the same point (x, y),

$$g(x, y) = Q[f(x, y)], \tag{1}$$

where Q is a "response operator" and is wavelength dependent. If the relative locations between a grid point (x, y) and a data point $(x + r\cos\theta, y + r\sin\theta)$ are as shown in Fig. 1, then the relationship between the true field and the filtered field may be expressed by

$$g(x, y) = \int_0^{2\pi} \int_0^{R_c} f(x + r\cos\theta, y + r\sin\theta) \times w(r, k) r dr d\theta \tag{2}$$

where $w(r, k)$ is a simple Gaussian low pass filter,

$$w(r, k) = [1/4\pi k] \exp(-r^2/4k). \tag{3}$$

The $4k$ is a parameter that determines the shape of the weighting curve and thus the influence accorded to observations at distance r from (x, y).

Figure 2 shows how the limits of integration apply to (2) when part of the area of integration overlaps the boundary of the data field. We will assume that a continuum of data exists to the left of the data boundary. We also assume that the integration is carried out to some scan radius R_c, $(R_c < \infty)$, beyond which the value of the weight function is some very small number so that truncation of the weight function at R_c will not noticeably affect the response characteristics. The interval of integration proceeds counterclockwise through the data-rich part of the scan area beginning at θ_1 and ending at θ_2. The remaining interval of integration covers the area where the scan area overlaps the data boundaries and includes the data-rich triangular area

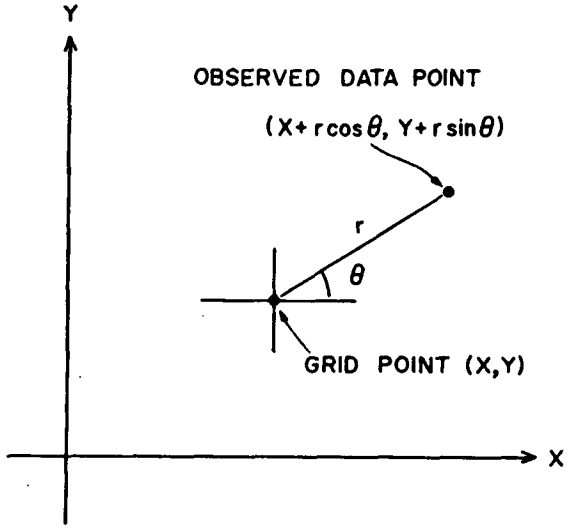

FIG. 1. Coordinate system used in objective analysis expressed by (1). Point (x, y) is conveniently chosen as a grid point of a square mesh; point $(x + r\cos\theta, y + r\sin\theta)$ represents one point where information is observed. Theoretically, these are continuously arrayed over the x–y plane, but in the practical application, they are discrete points, irregularly arrayed (after Barnes, 1973).

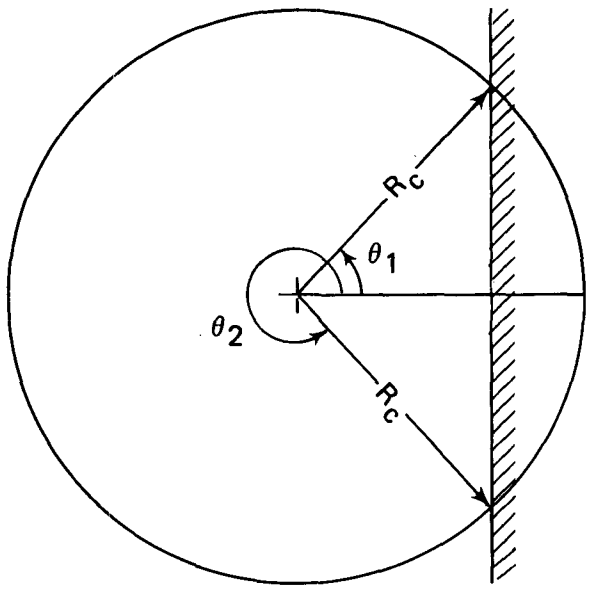

FIG. 2. Schematic showing the intersection of an influence area about a grid point with a data boundary.

with two sides bounded by R_c and the third side bounded by the edge of the data field.

In the event that the grid point is far enough removed from the data boundary, the integral reduces to the equation for the response for a data continuum over an infinite plane. Otherwise, a solution for (2) is difficult to obtain because the distance from the grid point to the data boundary is a function of the angle, θ. If $f(x, y)$ is an idealized monochromatic data field of the form $A \sin(ax)$ where $a = 2\pi/\lambda$, then $g(x, y)$ is determined by the weighted sum of the original function, $f(x, y)$, with the original function shifted 90 degrees out of phase,

$$g(x, y) = D(a, k)f(x, y) + E(a, k)h(x, y) \qquad (4)$$

where $h(x, y) = A \cos(ax)$. The amplitude responses, $D(a, k)$ and $E(a, k)$ are integrals of higher-order Bessel functions. Barnes (1964) presented the analytical solution for $D(a, k)$ for data distributed over an infinite plane. In his 1973 paper, he showed that $E(a, k)$ vanishes under the same conditions. These conditions are not satisfied near data boundaries and both integrals are nonzero. We have solved them numerically.

a. Theoretical response for a single data boundary

Throughout this development, a continuum of data within the boundaries of a finite data field (Fig. 2) is assumed. If $f(x, y)$ is specified, then the weight function shape parameter and the length of the wave are all that are required to find the responses $D(a, k)$ and $E(a, k)$. However, to better relate the theoretical results from (4) to distances measured from the edge of the data field, we introduce a length scale $S = \lambda^*/2$ where λ^* is a reference wavelength. The reference wavelength is chosen to equal the minimum resolvable wave, the final response of which must be prespecified in the GEMPAK method (Koch *et al.*, 1983). Thus, if the methods described here are applied to the analysis of real data, S is equivalent to the average spacing between discretely distributed observations.

The first-pass responses for the first term of (4) at selected distances from a data boundary are shown in Fig. 3a. Distances are given in fractions of S (S = 10 km). The shape of the weighting curve is $4k$ = 64, a value used by Barnes for the first-pass analysis of data distributed on the 1970 NSSL surface mesonetwork. The response for a grid point removed a distance, $2S$, from the data boundary is unchanged from the response for an infinite plane of continuous data for the range of wavelengths in Fig. 3a. At distance S from the boundary, the responses for the medium and long wavelengths are slightly less than the infinite plane responses—an indication that these waves receive additional damping due to boundary effects. Additional

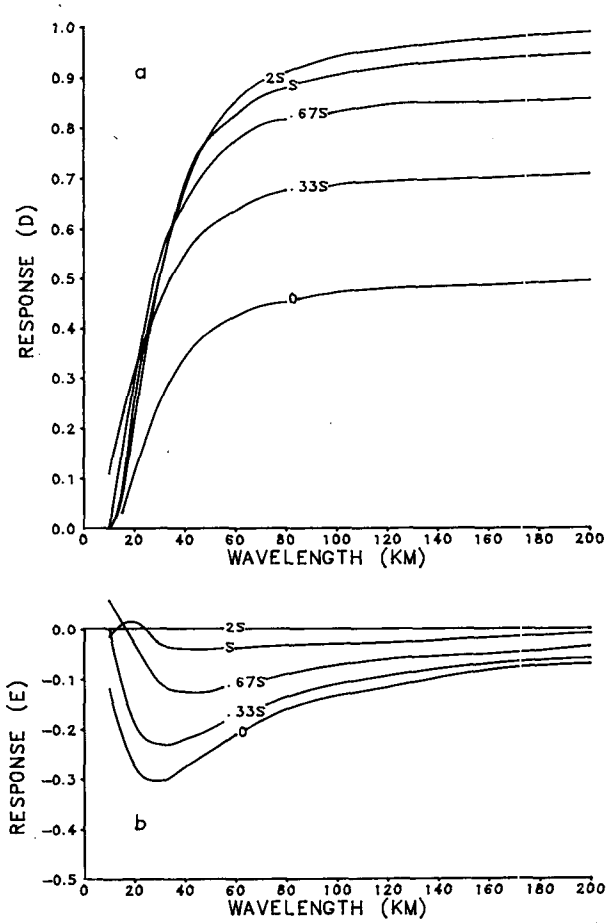

FIG. 3. (a) Responses for $4k$ = 64 for the first term of (4) at selected distances from the grid boundary. Distances from data boundary measured in fractions of S. (b) Responses for the second term of (4) for the same distances from the grid boundary.

smoothing is clearly implied for all wavelengths when the grid point is located at distances less than $0.67S$ from the data boundary. The Gaussian filter degrades the spectrum of waves to the extent that less than 50 percent of the amplitudes of the long waves are restored at the data boundary. Further, upon extending this analysis to very long waves, it is found that $D(a, k)$ approaches 0.5 in the limit as $\lambda \rightarrow \infty$.

Figure 3b shows how the second term of (4) shifts the phases of the waves near the data boundaries. Phase shifts are negligible at distances greater than S from the data boundary. Maximum phase shifts occur at the data boundary and for the short but resolvable waves in the range 20–60 km. Approximately 30 percent of the amplitude of the 30 km plane wave appears as a phase shifted wave at the data boundary.

The magnitudes of the impacts that the absence of data beyond the boundaries of a data field have upon filter fidelity at any location within an analysis grid are also dependent upon the shape factor $4k$. Figure 4 shows response curves for four values of $4k$ at a grid point located at a distance of $0.67S$ from the data boundary. The response for $4k = 16$ shows no significant impact because that part of the scan area where relatively large weights are accorded to the data does not overlap the data boundary. Thus, in a sense, the filter does not "see" the data boundary when $4k = 16$. A value of $4k = 205$ produces first pass response characteristics in both wave amplitude and phase shift at $0.67S$ similar to the response $4k = 64$ would produce at about $0.5S$ from the boundary (Fig. 3b). Since the larger $4k$ increase the effective scan areas, the deleterious impacts of the data boundary upon filter fidelity must increase in magnitude and must appear at greater distances into the grid interior because a greater percentage of the scan areas will overlap the data boundary.

The interpolation method may be modified to obtain the desired response at small wavelengths by applying correction pass(es) through the initial interpolation field. In application, we perform the nth pass by finding $g_{n-1}(x, y)$ through bilinear interpolation and then adding to the previous $(n - 1)$ pass field the smoothed residual difference between the observed data values and the $(n - 1)$th pass estimated values at the data location. Thus,

$$g_n(i, j) = g_{n-1}(i, j) + Q_n[f(x, y) - g_{n-1}(x, y)], \quad (5)$$

where the general response operator, Q_n, may or may not take on the same value as for the previous pass.

For reasons of computer economy, Barnes (1973) modified the original analysis technique so that only one correction pass through the data is required to achieve the desired response at small wavelengths. By this method, the filter is made to return more of the amplitude of the short waves through a reduction of the shape factor by a fraction, γ. This procedure is analogous to decreasing the influence radius for the

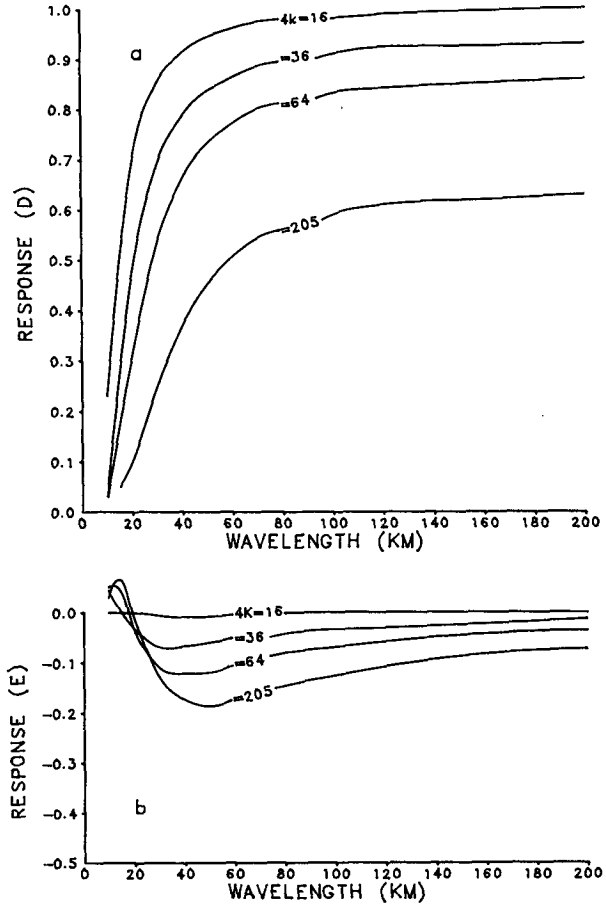

FIG. 4. Response for four values of $4k$ at a grid point location $0.67s$ from the data boundary.

Cressman (1959) analysis technique except that the number of observations within the scan area remains the same. Instead of reducing the number of observations, the weights are adjusted so that the relative importances of the observations closest to the grid point are increased on the correction pass. By this method, the estimated values at the grid points are given by

$$g(i, j) = D'f(x, y) + E'h(x, y) \quad (6)$$

where the final responses, D' and E', for the modified analysis method are given by

$$D' = D_0 + D_1 - (D_0D_1 - E_0E_1) \quad (7)$$

$$E' = E_0 + E_1 - (D_0E_1 + E_0D_1). \quad (8)$$

If a grid point is located at greater distance from the data boundaries, then $E_1 = E_0 = 0$, $E' = 0$ and D' reduces to the form given by Barnes (1973). Otherwise, the amplitudes of the phase shift term are nonzero where data boundaries influence the analysis. As E_0 and E_1 are related through γ, both are of the same sign, their product is always positive, and therefore the phase

shift excited at the first pass always increases the final response. The solid curves in Fig. 5a are examples of the final responses, D', after one correction pass at a point located at the data boundary. The value of $4k$ is 205 and is equal to the value of $4k$ for the first pass of the GEMPAK objective analysis. The correction pass value for γ is 0.2. The curve labeled $E = 0$ is the final response calculated with $E = 0$ and it serves as a baseline for evaluating the impact of the phase shift upon the final analysis. The data boundaries cause the method to restore only about 70 percent of the original long waves. A comparison of the two curves illustrates the importance of the phase shift terms in increasing the response for the short wavelengths in the range 30 to 60 km, the increases for these waves ranging from 6 to 10 percent. This is the range of waves for which the first pass response E_0 is greatest (see Fig. 4b for reference).

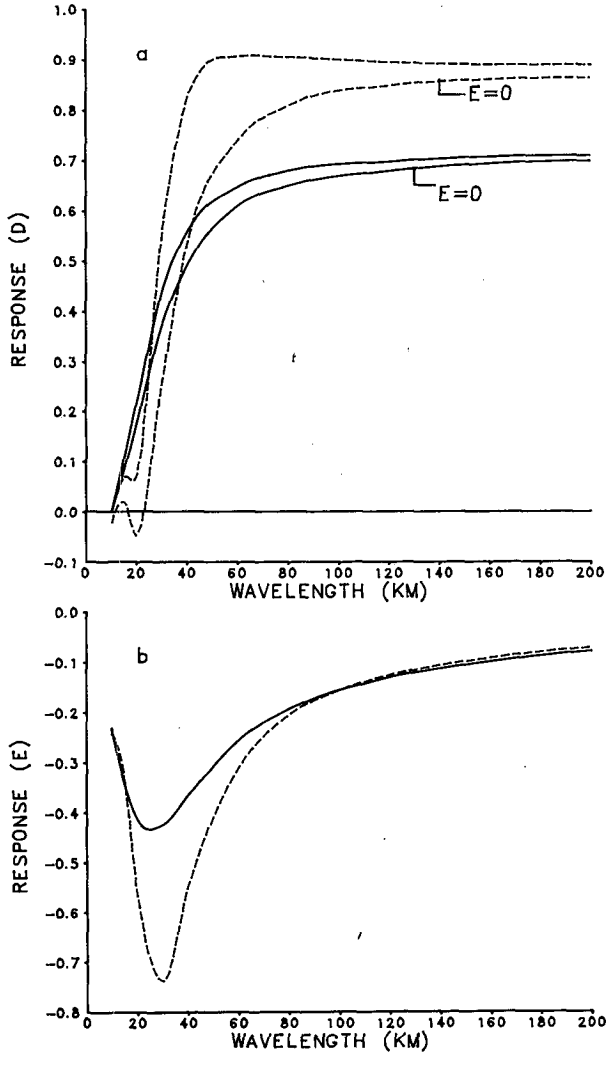

FIG. 5. (a) Final response, D', for $4k = 205$ at the data boundary. (b) Final response, E', for the same $4k$. Solid lines are responses for the one-correction pass method and dashed lines are responses for the three-correction pass method.

The tradeoff is that the data boundaries also excite large amplitude phase-shifted waves for the same range of waves near the data boundary (Fig. 5b). The maximum amplitude of the phase shifted waves occurs at the 30 km wave and is 43 percent.

It is expected that the impacts of the data boundaries will vary among objective analyses obtained by other methods or from the same method with different control parameters. The dashed curves in Fig. 5a are examples of the final responses, D', after three correction passes with the Barnes (1964) method. We set the shape factor $4k = 205$. A comparison between the dashed curve, labeled $E = 0$, and the two solid curves shows that this method substantially improves the fidelity of the Barnes filter near data boundaries for wavelengths greater than 40 km. Approximately 85 percent of the amplitudes of these waves are restored. Inclusion of the phase shift terms improves the fidelity of the filter still more with the greatest increases in the 30–60 km range. This is the range of waves for which the first pass response E_0 is greatest. These increases range from only 6 percent for the 20 km wave to 38 percent for the 40 km wave.

However, this analysis also produces large amplitude phase-shifted waves for the same range of waves near the data boundary (Fig. 5b). Seventy-five percent of the amplitude of the original 30 km wave appears as a phase shifted wave at the data boundary. More than 50 percent of the amplitudes of the 20 and 40 km waves are returned out of phase. Phase shifting is a lesser problem with the longer waves. Further, the amplitudes of these phase shifted waves and those obtained with the single correction pass method become negligibly small for all waves where the distances from the boundary of the dataset exceed S.

b. Theoretical response for limited-area datasets

The previous discussions have focused upon the impacts the single boundary of a data field have upon the filtering characteristics of the Gaussian weight function. We now turn to the limited-area dataset and consider that the response at *all* points within the small grid network may be impacted to some degree by one or more data boundaries. Keeping the numerical approximation to the general response equation, we modify the geometry of the data field by assuming that the data are distributed uniformly within a circle with a diameter equal to $2S$.

The final response curves for limited-area datasets (Fig. 6) are labeled in distances measured in fractions of S from a data boundary. They begin at the data boundary (0) and terminate at the center of the circle (S). The response curves are for the low-pass filter designed to produce the infinite plane response identical to the GEMPAK default criteria ($D_0 = 0.0064$ and

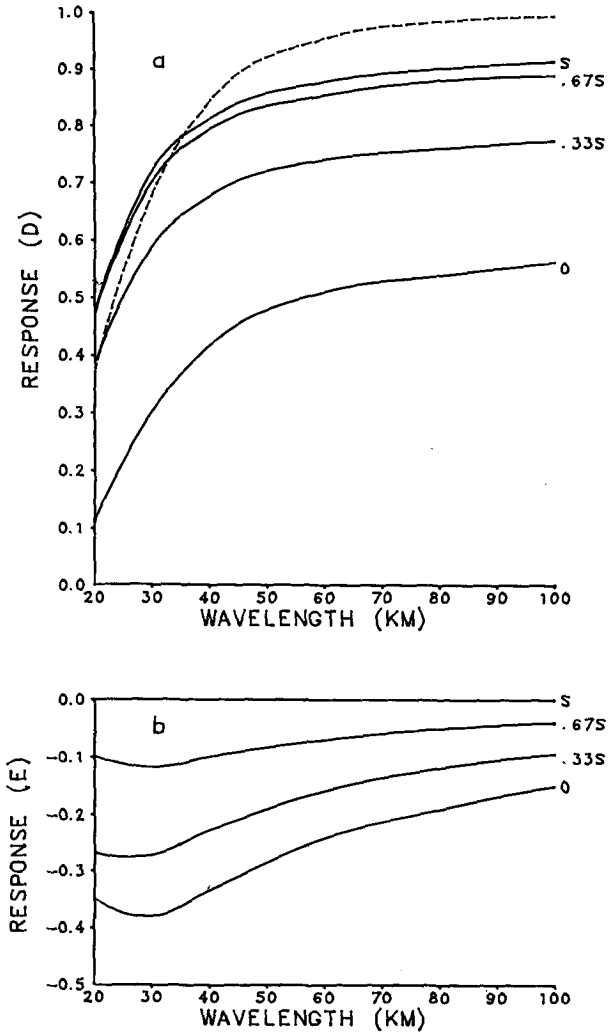

FIG. 6. Final response curves in fractions of S from the data boundary for a limited-area dataset. (a) Amplitude response, D' and (b) phase shift response, E'. Response curves obtained with GEMPAK default criteria.

$\gamma = 0.2$) at the $2S$ wavelength. When applied to the limited-area dataset, this weight function modifies the character of all of the waves studied (Fig. 6a). All of the longer waves are filtered. The filtering is most extensive at the data boundary; however, the amplitudes of long waves at the center of the data area also are reduced. Short waves are amplified by this analysis. Responses for the waves in the range from 20 to 40 km wavelength are increased above the infinite plane response calculated with identical parameters (dashed line). Maximum increases at the $2S$ wave (20 km) approach 10 percent at the center of the limited-area data field. These increases cannot be explained by the addition of the phase shift term in (14) because the data are distributed symmetrically about the central point. This satisfies the condition for the phase shift to vanish and the phase shift does vanish (Fig. 6b line labeled S). Instead, the short waves amplify because the influence area is truncated at the data boundaries. Moreover, the magnitude of the amplification depends upon the extent of truncation and hence upon the size of the limited-area data field. Figure 7 shows the differences between the truncated final response and the infinite plane final response for the $2S$ wave if R_c varies in the range from zero to $2S$. The differences increase from $-e^{-1}$ (the truncated final response is equal to zero if there is only one data point) to $+0.12$ if R_c is equal to approximately $0.67S$. The truncated final response approaches the final response for the infinite plane for $R_c \geq 1.67S$.

3. Examples of impact of data boundaries upon objective analyses

In this section, we use objective analyses to show that the impacts of data boundaries extend for significant distances into the grid interiors. The data locations are colocated with grid points on a 21 by 21 grid with a 3.175 km grid spacing so that there is no need for any additional interpolation to estimate values of the gridded fields at off-grid data locations. It also allows the direct comparison of the objectively filtered fields with the predictions of the response theory in section 2. The final filtered value at each grid point after L correction passes through the data is the weighted average of $M \times N$ observations plus the sums of the correction passes according to

$$g_L(i,j) = \frac{\sum_{m=1}^{M}\sum_{n=1}^{N} w_{0,m,n} f(m,n)}{\sum_{m=1}^{M}\sum_{n=1}^{N} w_{0,m,n}} + \sum_{l=1}^{L} C_l, \qquad (9)$$

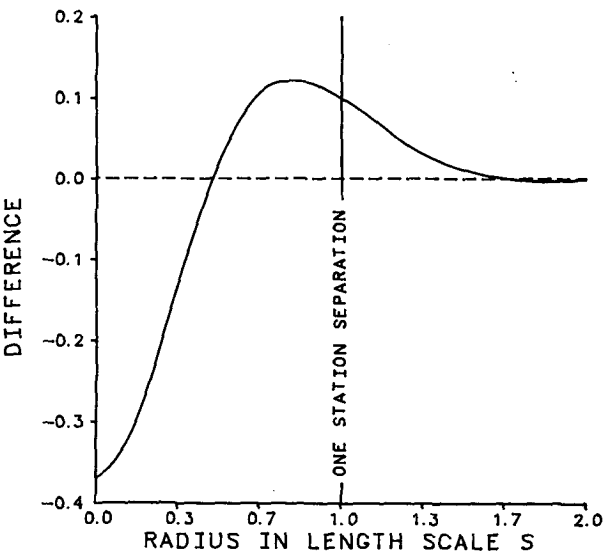

FIG. 7. Differences between truncated and infinite plane responses for the $2S$ wave for different sized data areas. Response curve obtained with GEMPAK default criteria.

where

$$C_l = \frac{\sum_{m=1}^{M}\sum_{n=1}^{N} w_{l,m,n}[f(m, n) - g_{l-1}(m, n)]}{\sum_{m=1}^{M}\sum_{n=1}^{N} w_{l,m,n}}. \quad (10)$$

The weight function, $w_{l,m,n}$ is given by

$$w_{l,m,n} = \exp[-r^2(m, n)/4k]. \quad (11)$$

The data are taken from analytic functions that include sloping plane surfaces and monochromatic waves ranging from 20 km through 80 km. We use either three correction passes with $w_{l,m,n} = w_{0,m,n}$ or the GEMPAK default criteria, one correction pass with $w_{1,m,n} = 0.2w_{0,m,n}$.

Figure 8 demonstrates the impacts of data boundaries on a three-correction pass analysis and upon a one-correction pass analysis for a 20 km monochromatic wave (Fig. 8a). The initial value for $4k$ was 205. Filtering the wave field by (8) with three correction passes does not restore this $2S$ wave (Fig. 8b). However, a phase-shifted wave of amplitude comparable to the amplitude of the original wave appears near the boundaries in accordance with the response theory developed in the previous section (compare with Fig. 8a). We subtract from the analysis in Fig. 8b a filtered wave determined from response theory for data distributed over an infinite plane. This leaves the phase-shifted wave as a remainder located near the boundary (Fig. 8c). The residual of 10 units corresponds to approximately 63 percent of the amplitude of the original wave. This compares favorably with theory, which predicts a phase-shifted wave with amplitude equal to 56 percent of the original wave (Fig. 5b). The one-correction pass analysis run with the GEMPAK default criteria restores e^{-1} of the amplitude of the original wave (Fig. 8d). Subtraction of the infinite plane component of this filtered wave also leaves a reversed phase wave nearly identical to the wave in Fig. 8c.

The analysis modeled after a limited-area dataset demonstrates that the absence of observations beyond the boundaries of the data field can have a significant impact over the whole analysis domain. We use a monochromatic 60 km wave for this part of the study. The wave is filtered with the one-correction pass method subject to GEMPAK default criteria, which assumes that this wave is equivalent to the minimum resolvable wave. We then subtract a filtered wave determined from infinite plane response as was done in developing Fig. 8c. The line (curve 1) in Fig. 9 shows that this filter draws boundary effects into the interior of the analysis. (If this wave is equivalent to the minimum resolvable wave then one station separation is equivalent to the length scale S.) The magnitudes of these boundary effects are in percentages of the amplitudes of the original wave and are in general agreement with predictions of theory. Decrease the initial $4k$ by a factor of 4 and (7) reduces the magnitude of the phase-shifted wave and concentrates it nearer the data boundary (curve 2). Increase the initial $4k$ by a factor of 4 to smooth out the undesirable boundary effects and (7) reduces the amplitude of the phase-shifted wave (at least for this 60 km wave) but draws the boundary effects into the grid interior (curve 3).

4. Discussion

Successive corrections objective analysis techniques have often been used to analyze (filter) data taken from limited-area networks onto a regular mesh without regard for the impacts upon the analysis in the interior of the grid caused by the absence of data beyond the boundaries of the network. The response theory for the Barnes objective analysis methods was extended to include boundary effects and was compared with objective analyses of analytic data. The analytic data was distributed semi-continuously over grid points of a fine scale mesh. Several important points regarding the objective analysis of limited area datasets were revealed through this study.

(i) Both the theoretical and the analytic studies showed that data boundaries can have a significant impact upon waves defined within the interior of an objective analysis. The most deleterious boundary effects were that the long waves were filtered and the short waves were phase shifted. Long waves suffered losses in amplitude of up to 50 percent. Up to 70 percent of the amplitudes of the short waves were restored out of phase. It was also found that, upon use of multiple-pass filtering, boundary effects amplified resolvable short wavelengths in the range from $2S$ to $6S$ relative to the responses predicted by theory for points unaffected by data boundaries. The causes for these relative amplifications were feedbacks from waves shifted out of phase on the first pass and/or truncation of the influence area by limited-area datasets. The magnitudes of the feedbacks from phase-shifted waves were sensitive to the wavelength. Relative amplifications ranged from about 6 percent for the $2S$ wave to 30 percent for both the $3S$ and $4S$ waves—an apparent increase in the filter fidelity of the Barnes methods near the data boundaries. The maximum relative amplification caused by the truncation of the influence area by small datasets occurred for the $2S$ wave and was approximately 12 percent.

(ii) The distance that boundary effects intruded into the interior of the grid was a function of the weight function shape parameter $4k$. Attempts to decrease boundary effects through a smooth analysis obtained by using large initial $4k$ actually drew boundary effects farther into the grid interior. Reducing $4k$ decreased and concentrated the boundary effects to near the grid boundaries. However, the analyst should be aware that a reduction of $4k$ modifies the response characteristics

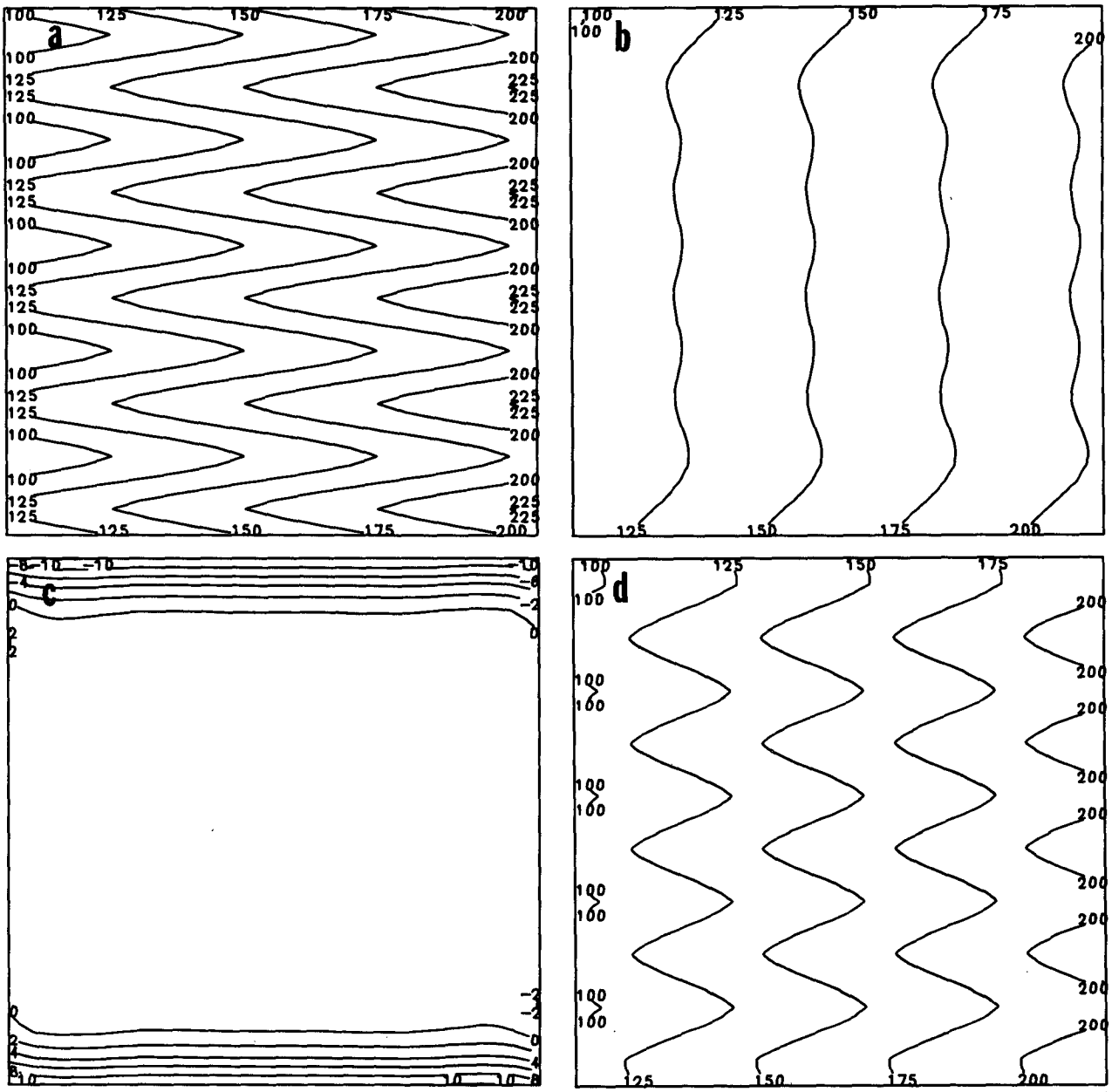

FIG. 8. (a) A 20 km $2S$ monochromatic wave used for analytical studies of boundary effects; (b) a three-correction pass Barnes analysis of the wave; (c) boundary impacts upon analysis; and (d) analysis of same wave with GEMPAK default criteria.

to permit short wavelengths, a tradeoff that may cause phase changes and aliasing of waves within the interior of the grid if the observations are unevenly spaced.

(iii) After the analytic tests were performed with realistic values for $4k$, such as the GEMPAK default criteria, it was found that boundary effects intruded into the interior of the analysis domain a distance equal to roughly one half the length of the wave. If the wave is the minimum resolvable wave, then this distance is equivalent to the average separation between observations. This poses no serious problem for the analysis of large datasets. The analysis area can be designed so that some data fall outside the grid, or so that several rows and columns of the grid can be discarded after the analysis. This latter approach has been proposed by Koch *et al.* (1983). These options are not always possible for the analysis of limited-area datasets; there may not be enough observations. The analyst must be prepared to accept that the data boundaries will modify the response characteristics within the interior of the analysis domain. For example, if a limited-area dataset consists of nine evenly spaced observations sited so

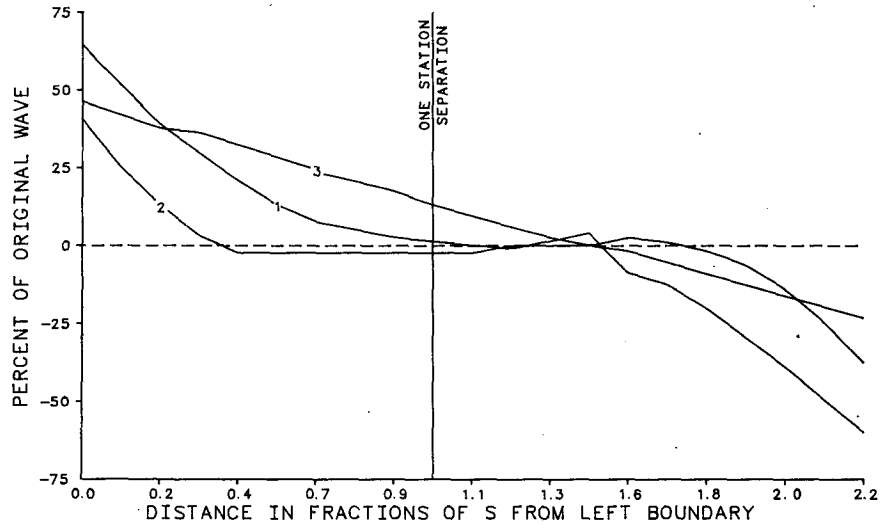

FIG. 9. Cross section along a 60 km wave used for three objective analyses of analytical limited-area data field. Boundary effects expressed as percentages of the amplitude of the original wave.

that eight stations form the boundary and one station is at the center of the network, and if boundary effects penetrate to a distance equal to the average station spacing, then all of the domain will suffer to some extent from boundary impacts.

(iv) The analysis presented here is a "worst case scenario" with regard to the phase of the original function $f(x, y)$ in determining the final response for the Barnes filter near data boundaries. Our investigation of the phase-shift term of (4) revealed that, if $f(x, y) = A\cos(ax)$, then the phase-shifted wave is $h(x, y) = A\sin(ax)$. This wave vanishes at the data boundary where $x = 0$. In addition, it was found that the integral, $E(a, k)$, changes sign when $f(x, y) = A\cos(ax)$. It follows, therefore, that $E(a, k)$ must decrease to zero somewhere within the range of phases 0 to $\pi/2$ for the original wave. Thus the maximum magnitudes for both $E(a, k)$ and $h(x, y)$ are permitted where $f(x, y) = A\sin(ax)$.

(v) Throughout this discussion, it has been assumed that a continuum of information exists within the limited area domain. The analysis of analytic data has been carried out with a densely distributed regularly spaced data field. A data continuum was approached for some waves. We have emphasized that the results herein are the best that can be expected for the Barnes analysis schemes. In the real world, the data are arrayed discretely and the data distribution further degrades the response to the filtering process. If the data are not evenly distributed, then phase changes and a higher "noise" level are inherent to the analyzed field. We have not emphasized the analysis of unevenly spaced data because these degrading factors are dependent upon the data—the phenomena represented by the data, the data distribution, and the boundaries of the data field. And, when the observation platform is suspended within the wind field, the data distribution and the boundaries of the data field are variables determined by the phenomena represented by the data.

In conclusion, consider the applications of limited-area datasets from field programs designed for the investigation of mesoscale and/or regional scale phenomena. If the purpose of a limited area network is the acquisition of information on the spatial distribution of meteorological variables, including gradients of the wind field, the analyst should be prepared to accept that most (probably all) of the analyses will suffer to some extent from the impacts of the boundaries of the data field. It should be kept clear, however, that the above conclusion is based upon the results of an investigation with the Barnes objective analysis schemes. An improved objective analysis scheme that concentrates boundary effects to near the grid boundaries and produces what can be called a "good analysis" in the interior of a limited area domain is essential to provide an accurate description of the local structure of the atmosphere with a limited area data field.

Acknowledgments. This research was supported by NASA under contract NAS8-34902. Ms. Rebecca Runge is acknowledged for typing the manuscript.

REFERENCES

Alberty, R., J. Weaver, D. Sirmans, J. Dooley and B. Bumgarner, 1977: Spring Program '76. NOAA Tech. Memo. ERL NSSL-83. 130 pp. [NTIS PB2807451AS.]

Barnes, S. L., 1964: A technique for maximizing details in numerical weather map analysis. *J. Appl. Meteor.*, **3**, 396–409.

——, 1973: Mesoscale objective analysis using weighted time-series observations. NOAA Tech. Memo. ERL NSSL-62, 60 pp. [NTIS COM-73-10781].

——, J. H. Henderson and R. J. Ketchum, 1971: Rawinsonde observation and processing techniques at the National Severe

Storms Laboratory. NOAA Tech. Memo. ERL-NSSL-53, 246 pp. [NTIS COM-71-00707.]

Changnon, S. A., Jr., F. A. Huff and R. G. Semonin, 1971: METROMEX: An investigation of inadvertent weather modification. *Bull. Amer. Meteor. Soc.*, **52,** 958–967.

Cressman, G. P., 1959: An operational objective analysis system. *Mon. Wea. Rev.*, **87,** 367–374.

Doviak, R. J., 1981: 1980 Spring Program Summary. NOAA Tech. Memo. ERL NSSL-91, 124 pp. [NTIS PB81-234940].

Eddy, A., 1964: The objective analysis of horizontal wind divergence fields. *Quart. J. Roy. Meteor. Soc.*, **90,** 424–440.

Gandin, L. S., 1963: *Objective Analysis of Meteorological Fields.* Translated by Israel Programme for Scientific Translations, Jerusalem, 242 pp.

Hill, K. G., S. Wilson and R. E. Turner, 1979: NASA's participation in the AVE-SESAME '79 program. *Bull. Amer. Meteor. Soc.*, **60,** 1323–1329.

ISWS, 1974: Project METROMEX: An overview of Illinois State Water Survey Projects. *Bull. Amer. Meteor. Soc.*, **59,** 89.

Koch, S. E., M. DesJardins and P. J. Kocin, 1983: An interactive Barnes objective map analysis scheme for use with satellite and conventional data. *J. Climate Appl. Meteor.*, **22,** 1487–1503.

News and Notes, 1981: CCOPE begins Spring 1981. *Bull. Amer. Meteor. Soc.*, **62,** 683–684.

Schlatter, T., 1975: Some experiments with a multivariate statistical objective analysis scheme. *Mon. Wea. Rev.*, **107,** 458–476.

Stephens, J. J., 1967: Filtering responses of selected distance-dependent weight functions. *Mon. Wea. Rev.*, **95,** 45–46.

——, and J. M. Stitt, 1970: Optimum influence radii for interpolation with the method of successive corrections. *Mon. Wea. Rev.*, **98,** 680–687.

Taylor, W. L., 1982: 1981 Spring Program Summary. NOAA Tech. Memo. ERL NSSL-93, 97 pp. [NTIS PB82-244757].